NASA Contractor Report 3071

Prediction of Compliant Wall Drag Reduction

Part II

Steven A. Orszag

CONTRACT NAS1-14906
JANUARY 1979

NASA

NASA Contractor Report 3071

Prediction of Compliant Wall Drag Reduction

Part II

Steven A. Orszag
Cambridge Hydrodynamics, Inc.
Cambridge, Massachusetts

Prepared for
Langley Research Center
under Contract NAS1-14906

NASA
National Aeronautics
and Space Administration

Scientific and Technical
Information Office

1979

SUMMARY

A numerical model of turbulent boundary layer flows over compliant walls has been investigated. The model is based on Burton's observation that outer flow structures in turbulent boundary layers produce large pressure fluctuations near the wall. Wall streaks undergo space-time retardation due to this convected adverse pressure gradient; a new burst appears when the velocity profile becomes highly inflectional. The idea of the model is that the wall motion can possibly interrupt this feedback loop of burst formation long enough for the favorable gradient part of the pressure pulse to effect a decrease in the burst frequency. This model is attractive because it addresses the pre-breakup part of the burst cycle which is likely the easiest part of the cycle to affect externally and, hence, affect burst frequency. The results of our calculations indicate that certain small wavelength wall motions can have a significant effect upon the stability of turbulent boundary layers. This result suggests that novel structural dynamics will be an essential component of successful drag reduction by compliant walls.

1. INTRODUCTION

In this report, we discuss the formulation, development, and some applications of a numerical model of the effect of compliant walls on turbulent boundary layer flows. Since skin-friction drag accounts for about half the drag on long-haul aircraft, any reduction in this drag is of great importance in improving fuel economy and aircraft range as well as increasing payload efficiency and decreasing environmental pollution.

The current state of experimental and theoretical research on compliant walls and their effect on turbulent boundary layers has been reviewed by Fischer, Weinstein, Ash & Bushnell[1] and by Bushnell, Hefner & Ash[2]. In summary, the current state of both experiments and theory is inconclusive. Some experiments show a substantial effect of compliant walls on drag, while others do not. It is not clear whether conventional materials can serve as suitable compliant boundaries to give drag reduction, though there do seem to be some attractive possibilities. It is only clear that drag reduction by compliant walls is not as simple a phenomenon as may be suggested by cursory consideration of the hydrodynamical efficiency of dolphins[3]. Evidently, the dynamical characteristics of the wall are crucial in determining whether drag reduction or drag enhancement will result; the response of the wall must be matched in some dynamical sense

still to be elucidated to the characteristics of the turbulent boundary layer over it. One of the principal purposes of the present work is to help in identifying the nature of the effect of the wall motions on the drag so that design of suitable walls can be expedited.

There have been several theoretical investigations of turbulent boundary layer flows over moving walls; a survey is given in Ref. 2. One of the most attractive ideas[2] for explaining the drag reduction by compliant walls is that the wall influences the turbulent burst phenomenon by providing a pressure field that tends to inhibit bursts when they normally occur. This idea leads to significant qualitative understanding of the effect of compliant walls. In this paper, we discuss a numerical model based on the above idea and report quantitative tests of it as a mechanism of compliant wall drag reduction.

In Sec. 2, we discuss the proposed mechanism of compliant wall drag reduction. In Sec. 3, we discuss the numerical model of the mean flow motion. Then, in Sec. 4, we discuss techniques for the investigation of the stability of the predicted mean flow profiles and for the prediction of burst frequency. In Sec. 5, we present results of the present model for turbulent boundary layer velocity profiles during the burst phenomenon and use these results to fix various parameters of the model by comparison with experimental results. Then, in Sec. 6, we present numerical results for the combined mean-flow and stability analysis of the turbulent boundary layer flow over a compliant wall. In this analysis, we use a crude burst predictor based on amplification factors. Finally, in Sec. 7, we summarize the current state of research on the turbulence flow model investigated here.

2. A PROPOSED MECHANISM OF COMPLIANT WALL DRAG REDUCTION

In the last decade, there has accumulated a wealth of experimental evidence that the process of burst formation in turbulent boundary layer flows is not completely random, but rather can be correlated with a set of reasonably well-ordered dynamical events. Thus, a plausible sequence of coherent events for formation and regeneration of bursts is as follows:[4-6]

1. Large outer structures produce a large adverse pressure pulse that moves at a speed of roughly $0.8U_\infty$ and has an amplitude of roughly $3p'_{rms}$, where p'_{rms} is the rms wall pressure intensity.

2. The combination of the adverse part of the pressure pulse and an imposed wall-ward velocity creates highly

inflectional velocity profiles in the wall region.

3. The inflectional velocity profiles are highly unstable and tend to produce new bursts.

4. The favorable part of the pressure pulse due in some way to previous bursts tends to assist the new burst in 'sweeping' out away from the wall. Most of the Reynolds stress and turbulence production occurs during the burst and sweep process, with relatively low turbulence activity between bursts. The Reynolds stress is about 50 times the average value during the burst process.

Bushnell[2] has proposed that the above sequence of events can be used to formulate a quantitative flow model for the prediction of properties of turbulent boundary layers. The idea is to impose the experimentally measured pressure pulse due to 'old' bursts, to model the background turbulence between bursts using a crude turbulence model, and then to calculate the inflectional mean-velocity profiles produced by the pressure pulse using a two-dimensional Navier-Stokes equation computer code. Finally, the occurrence of new bursts can be investigated in this flow model by calculating the growth of Tollmien-Schlicting waves and using a amplitude-growth criterion[7] to predict the onset of new bursts.

Bushnell's turbulent boundary layer model also suggests a mechanism for drag reduction by compliant walls. If the wavelength of the wall motions is small (at most the wavelength of the imposed pressure pulse), the wall motion can interrupt the feedback loop outlined above somewhere between steps 2. and 4. If the short wavelength wall motions can delay burst formation through the adverse part of the imposed pressure pulse, then the favorable part of the imposed pressure pulse may inhibit bursting. In this case, turbulence production and turbulent boundary-layer drag are reduced.

The present work is motivated by the above ideas of Bushnell[8]. The model seeks to determine quantitatively whether realistic wall motions and imposed pressure pulses interact in a time-dependent environment in such a way as to decrease burst frequency and wall drag. We investigate numerically the mean velocity profiles produced by the imposed pressure pulse. We use two techniques to investigate the stability of the resulting profiles (see Sec. 4): 1) local quasi-steady analysis via the Orr-Sommerfeld equation and 2) study of the full linearized Navier-Stokes equations.

It seems that if the wavelength of the wall motions is large (of order the length of the imposed pressure pulse), there is no drag reduction. However, if the wavelength of the wall motions

is small (at most several sublayer thicknesses), drag reduction may occur. Future work must test the flow model further, particularly with respect to parameter sensitivity and three-dimensional effects (neglected here).

3. NUMERICAL MODEL FOR THE MEAN FLOW

In this Section, we discuss the numerical techniques used to solve the equations of Bushnell's turbulent boundary layer model discussed in Sec. 2. We solve the two-dimensional Navier-Stokes equations with a background turbulence model, inflow-outflow boundary conditions, and imposed inflow velocity and large-scale pressure pulse at 'infinity'. The resulting mean-flow profiles show the effect of the pressure pulse and inflow velocity in distorting (retarding) the mean profiles and in producing inflectional profiles.

The two-dimensinal Navier-Stokes equations for incompressible flow are

$$\frac{\partial \vec{v}}{\partial t} + \vec{v}\cdot\vec{\nabla}\vec{v} = -\vec{\nabla}p + \vec{\nabla}\cdot\underset{\approx}{T} + \vec{f} \ , \tag{3.1}$$

$$\vec{\nabla}\cdot\vec{v} = 0 \ , \tag{3.2}$$

where $\vec{v}(x,y,t)$ is the two-dimensional velocity field, $p(x,y,t)$ is the pressure, $\underset{\approx}{T}$ is the stress tensor, and $\vec{f}$ is an imposed external force. We solve (3.1) in a channel: $0 \le x \le L$ and $0 \le y \le H$. In a typical run, the values of L and H are $L = 600$ and $H = 200\text{-}400$ in units non-dimensionalized by the length ν/U_τ where U_τ is the friction velocity and ν is the viscosity.

We approximate the stress tensor $\underset{\approx}{T}$ by retaining only its x-y component:

$$T_{xy} = -\overline{u'v'} + \nu\frac{\partial \overline{U}}{\partial y} \ , \tag{3.3}$$

where ν is the viscosity, $\overline{U}$ is the mean velocity, and u' and v' are the x and y components, respectively, of the velocity fluctuations. The Reynolds stress, $-\overline{u'v'}$, is then evaluated by Van Driest's empirical formula[9] so that

$$T_{xy} = \left[B(.4y)^2 \left|\frac{\partial \overline{U}}{\partial y}\right| \left(1-e^{-Ay U_\tau/\nu}\right)^2 + \nu\right] \frac{\partial \overline{U}}{\partial y} \tag{3.4}$$

where the constant A is chosen to be 0.04 in agreement with experimental measurements of turbulent boundary-layer mean-velocity profiles. The constant B is an *ad hoc* correction to the usual Van Driest formula that accounts for the fact that the turbulence level between bursts is small; a typical value for the constant B in our calculations is $B = 0.05$.

Boundary conditions

The boundary conditions to be imposed on (3.1-2) require detailed consideration. Each of the four boundaries $x = 0, L$ and $y = 0, H$ poses its own special kind of boundary condition problem. A detailed analysis of these boundary conditions has been given in a preliminary version of this paper[10] and will not be repeated here. Our conclusions are as follows:

$x = 0$

Here the flow is assumed to enter the computational domain. Since the boundary is an inflow boundary, it is both physically and mathematically reasonable to assume that both components of the velocity field are known at $x = 0$. Thus, we assume that $u(0,y,t)$ and $v(0,y,t)$ are known for all y and t.

$x = H$

This boundary is an outflow boundary. Since the only non-vanishing component of the Van Driest Reynolds stress tensor (3.4) that we retain is T_{xy}, it follows that the Navier-Stokes equations (3.1-2) are parabolized in the x direction. Therefore, only the outflow component of the velocity, $u(L,y,t)$, need be imposed.

However, imposition of boundary values on $u(L,y,t)$ directly will give some difficulty because it will generate boundary layers near the outflow point $x = L$. Therefore, we impose the weaker boundary condition

$$u_{xx}(L,y,t) = 0. \tag{3.5}$$

Boundary conditions like (3.5) are known to have small upstream influence so they do not disturb the main region of computation which is away from the downstream boundary $x = 1$.

$y = 0$

This is the location of the compliant wall. If the wall were rigid, we would impose the boundary conditions

$$u(x,0,t) = v(x,0,t) = 0. \tag{3.6}$$

There are two effects of a moving boundary at $y = 0$. First, the boundary location is shifted to $y = \eta(x,t)$. Second, the wall motion as a function of t requires that the relative fluid velocity at the wall vanish, not the fluid velocity itself.

We impose boundary conditions at the moving wall by assuming linearized wall motion. This assumption is a great simplification and is justified because the wall motions of interest are not large compared to the sublayer thickness. [A modified version of the mean flow code is now being developed to handle nonlinear wall boundary conditions using techniques for fast conformal transformation recently developed by the author.] It follows that the vertical wall motion is

$$v = \frac{D\eta}{Dt} = \frac{\partial \eta}{\partial t} + U \frac{\partial \eta}{\partial x} , \qquad (3.7)$$

where $U = Dx/Dt$ is the component of the wall motion in the direction tangent to the wall. Eq. (3.7) for the vertical wall motion is true nonlinearly. Linearization of the wall motion implies that all quantities in (3.7) may be evaluated at the undisturbed wall location $y = 0$.

In order to complete the specification of boundary conditions at $y = 0$, it is necessary to know $U(x,t)$, the tangential component of the wall motion. This quantity depends on the physical model of the compliant wall, and must be specified in addition to the vertical wall motion $\eta(x,t)$. Thus, if the wall motion is achieved by physically sliding the boundary in the x-direction, then U will be non-zero and significant. On the other hand, if the wavy wall motion is obtained by means of suitably phasing the vertical wall motion with no concomitant x-motion then $U = 0$. In the present work, we do not determine the wall motions self-consistently, in the sense that we impose $\eta(x,t)$ and do not determine the effects of wall pressure fluctuations due to the turbulent boundary layer flow on the motion of the wall.

Most of the materials of current interest for compliant wall drag reduction applications are flexible materials that can 'stretch' in the y-direction but have little lateral freedom for movement in the x-direction. Therefore, because of the lack of specific information on this point, we have chosen the wall boundary condition to be $U = 0$. Admittedly, this is oversimplified, but a detailed model of the wall is necessary before this boundary condition can be improved.

It is not generally recognized that both $\eta(x,t)$ and $U(x,t)$ must be specified to determine the wall motion. However, consider the simple wall motion $y = \eta(t)$, independent of x. The motion of the wall motion $y = \eta(t)$, can be arbitrary and

the proper tangential boundary conditions are $u(x,\eta,t) = U(x,t)$.

$y = H$

The boundary conditions imposed at the top of the boundary layer $y = H$ are the most unusual, and the most difficult to get right. In order to model the large-scale pressure pulse due to old bursts, we want to impose the value of the pressure $p(x,H,t)$ at the top of the layer. According to the mathematical analysis of flow boundary conditions, the pressure $p(x,H,t)$, and the normal velocity, $v(x,H,t)$ may be specified *if* the boundary $y = H$ is an inflow boundary.

On physical grounds, we expect the magnitude of the normal velocity at the top of the layer to have profound effects on our ability to model the bursting process. In fact, we have found by numerical experimentation with the model (see Sec. 5) that there is strong sensitivity of the model to $v(x,H,t)$. We have assumed that

$$v(x,H,t) = - V \tag{3.8}$$

where V is a non-negative constant.

The imposition of the boundary conditions that $p(x,H,t)$ and $v(x,H,t)$ are specified has proved satisfactory in practice, except for some slight difficulty near the intersection of the outflow boundary $x = L$ and the lid $y = H$; this difficulty is evidently due to a very thin outflow boundary layer and was cured by introducing additional dissipation locally.

Another difficulty with the top boundary conditions was encountered first in running computations with compliant walls with wavelengths intermediate between the sublayer thickness and the pressure pulse wavelength. An instability developed that was evidently due to the interaction of wall pressure fluctiations produced by the moving boundary at $y = 0$ with the imposed pressure pulse at $y = H$. This problem was solved by implementing a variable grid map[11] in the y-direction to allow larger values of H with the same number of degrees of freedom in y. Thus, by moving the lid from $y_+ = 200$ to $y_+ = 400$, all trace of the previous instability was removed.

Numerical methods

Eqs. (3.1-2) with the boundary conditions discussed above have been solved using a mixed spectral-finite difference method. The vertical (y) direction is resolved using expansions in Chebyshev polynomials, while the x-direction is resolved using a second-order staggered-grid finite-difference scheme. Thus, in the unmapped case, we represent the velocity field by

$$v(j\Delta x,y,t) = \sum_{n=0}^{N} u_n(j\Delta x,t)T_n(2y/H-1) \qquad (3.9)$$

where Δx is the grid separation in x and $T_n(y)$ is the Chebyshev polynomial of degree n. A detailed review of the spectral and finite-difference methods used here has been given elsewhere[12,13].

We use Adams-Bashforth time differencing of the nonlinear terms, together with a semi-implicit time differencing scheme for the diffusive terms of the Van Driest Reynolds stress and for the inflow terms at $y = 0$ and $y = H$. Because the Chebyshev polynomial expansions have so much resolution at the top and bottom of the channel, they would give extremely stringent time-step restrictions on the Adams-Bashforth scheme. The semi-implicit method avoids these time-step restrictions[13].

The code is also formulated in such a way that a moving coordinate system in x can be used as an option. This option is not used, however, in the calculations reported in Sects. 5-6.

4. NUMERICAL METHODS FOR STABILITY CALCULATIONS

Once the mean flow profiles are calculated by the computer code described in Sec. 3, we study the stability of the resulting flow in two ways. We solve the Orr-Sommerfeld equation for temporally growing disturbances in steady, plane-parallel two-dimensional incompressible flow, and we also solve the linearized Navier-Stokes equations. The first procedure involves three important approximations. First, we calculate only temporally growing disturbances, so we must convert between temporal growth and spatial growth using a complex group-velocity transformation[15]. In some early calculations, we were even cruder; instead of the group-velocity transformation in Runs 1-7 reported below, we transformed using the phase velocity instead of the group velocity. Later runs have all used the group velocity transformation.

Second, by assuming the mean-flow to be steady we neglect possibly very important phase-coherence effects which could strongly affect growth rates. In the Orr-Sommerfeld stability analyses, time variation of the mean flows is included only by using different mean profiles at different times in the evolution of a wave packet. The justification for the approximation of steady flow is weak *a priori*; *a posteriori*, the results of the linearized Navier-Stokes analysis seem to agree well with the

local quasi-steady analysis. However, we have made a detailed comparison only in one case to date and this agreement may be fortuitous. The third approximation of the Orr-Sommerfeld stability analysis is the assumption that the flow is plane parallel in x; this defect is also remedied in the linearized Navier-Stokes calculations.

The Orr-Sommerfeld equation is solved by expanding the eigenfunction in a series of Chebyshev polynomials and then applying either global QR matrix eigenvalue routines or local Rayleigh quotient iteration routines. These procedures are very efficient and accurate[16,17].

The results of the linear stability analysis are used to predict the occurrence of a burst as follows. First, we calculate the stability characteristics of various profiles at a fixed location x and various values of the time t. These calculations proceed until a time t_0 is found at which the profile is unstable. From that time onwards, we calculate the amplification ratio by the formula

$$\frac{A}{A_0} = \exp \int \mathrm{Im}\, \omega/c_g \, dx \ , \tag{4.1}$$

where c_g is the complex group velocity of a mode with wavenumber and (complex) frequencey ω. The profiles whose stability is calculated are related in space-time by following a wavepacket using the relation

$$\Delta x = \mathrm{Re}(c_g)\, \Delta t \ . \tag{4.2}$$

Next, the Michel-Smith criterion[7] for occurrence of a burst is applied; a burst is presumed to occur if

$$\frac{A}{A_0} \gtrsim e^M \tag{4.3}$$

where M is a number of order 10. This empirical correlation has worked well for a variety of transition flows, but it is very crude and the number M that best fits experimental data may vary over the range 5-15 or wider[18].

We have also developed a computer code for solution of the linearized Navier-Stokes equations. Presently, the code solves the linearized Navier-Stokes equations using a Fourier series representation of the flow field in x and a Chebyshev series representation of the flow field in y, with rigid boundary conditions imposed at the wall $y = 0$ and the lid $y = H$ and periodic boundary conditions imposed at $x = 0$ and $x = L$.

Another linearized Navier-Stokes code is under development that allows imposition of inflow-outflow boundary conditions in x, as described in Sec. 3. The present linearized Navier-Stokes code is a linearized version of a full Navier-Stokes code used by the author and L. Kells to study transition and turbulence in planar shear flows[19].

The linearized Navier-Stokes equation code is currently being used in the following way. The mean-flow code is used to generate a set of mean velocity profiles for all x at a time t when the pressure pulse has propagated through a distance $L/2$. The profiles used in the linearized Navier-Stokes code at later times is obtained by convecting this fixed set of velocity profiles through the grid at a speed equal to the phase speed of the pressure pulse. (We have also made a run using the speed U and the results changed by less than 15%.) The evolution of a mode of the linearized equations is then studied as a function of time for a fixed x. The motivation for this somewhat contrived procedure is simply to minimize the amount of data handling. A combined code that marries the mean flow code to the stability analyzer with no external data transfers is under development.

5. FLAT PLATE RESULTS

In this Section, we report a number of numerical experiments performed to tune the Bushnell turbulent boundary layer model for flor over a flat plate. First, in Fig. 1, we show the results of a numerical experiment performed to test the accuracy of the Van Driest Reynolds stress (3.4) with $B = 1$ (full strength) in reproducing a turbulent boundary layer mean-velocity profile. The calculation (as well as other calculations reported in this paper) used 33 Chebyshev polynomials to resolve the boundary layer (y) direction and 257 staggered grid points to resolve the downstream (x) direction. For the experiment (Run 1) plotted in Fig. 1, we impose the boundary conditions $p = v = 0$ at $y_+ = H - 200$. It is apparent from Fig. 1 that a turbulent boundary layer profile is well preserved in evolution from the upstream boundary at $x = 0$ to $x_+ = 600$ is minimal -- in fact, no appreciable upstream influence of the boundary at $x_+ = 600$ is discernible beyond $x_+ = 500$.

The next set of runs were designed to adjust the background turbulence level constant B in (3.4) and the inflow velocity $-V$ at $y_+ = H$, as well as to test the form of the required pressure pulse to achieve reasonable mean velocity profiles. The goal of these experiments is to match the development of turbulent boundary layer profiles between bursts as measured by

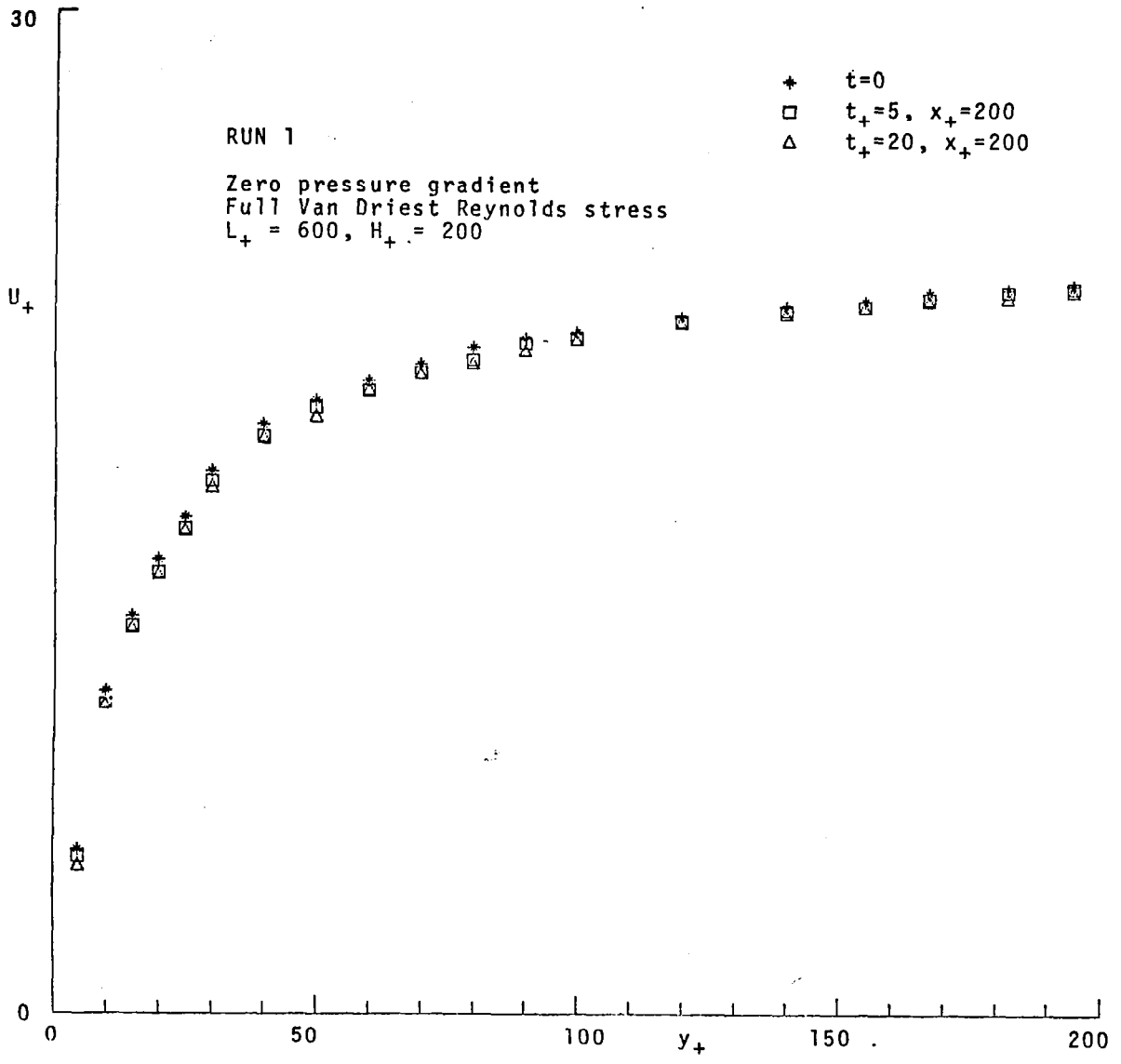

Figure 1. A plot of the calculated mean-velocity profiles for Run 1.

Blackwelder & Kaplan[20]. Some of the experimental data for conditionally averaged velocity profiles before, during, and after the period of burst formation are shown in Fig. 2. Observe the very strong inflectional profiles at a time delay of -3.1 ms. This profile is strongly unstable and gives rise to a burst a short time later.

In Fig. 3, we plot the form of the pressure pulse used in our calculations of the Bushnell model. The magnitude of the pulse is chosen to be $3p'_{rms}$, in agreement with Burton's data[4] and to occur over a time period of 25 (in units of ν/U_τ^2). The triangular form of this pulse is an arbitrary choice, but it is not inconsistent with available experimental data. In some of the numerical experiments reported below, the amplitude of the pressure pulse is $2.5p'_{rms}$ and in some others the length of the pulse is decreased to 20.

In Fig. 4, we plot the results of a numerical calculation using the code described in Sec. 3 with $B = 0.05$ and $v = 0$ at $y_+ = H$, together with the imposed pressure pulse. The agreement with the Blackwelder profiles shown in Fig. 2 is not very good.

In Fig. 5, we plot the results of a similar experiment in which the vertical dimension is truncated to $H = 100$ with the pressure pulse applied at $y_+ = 100$. The agreement with the experimental data is even worse. We conclude from this comparison that the pressure pulse must be imposed in the region $y_+ = 200$ and certainly not so close to the wall as $y_+ = 100$.

In Fig. 6, we plot the results of a claculation similar to that shown in Fig. 4, except that the imposed inflow velocity at the top of the layer is $v_+ = -0.5$ ($V = 0.5\ U_\tau$). In this case, the retardation due to the imposed pressure pulse is much larger than that shown in Fig. 4 and 6, except that the inflow velocity at the top of the layer is $v_+ = -2$. In this case, the inflect ionalprofile is very strong and even our two-dimensional mean-flow code with background turbulence model went unstable near the peak of the adverse pressure gradient pulse. This difficulty with Run 5 (shown in Fig. 7) is, we believe, unrelated to the calculational difficulties with the unmapped grid for intermediate wavelength compliant wall problems discussed in Sec. 3. We believe that the breakdown of Run 5 is due to the small value of $B = 0.05$, so that the background turbulence cannot stabilize (by diffusion) the unstable profile produced by the pressure pulse.

The conclusion to be drawn from Figs. 4-7 is that the strength of the inflectional profiles produced by the passage of the pressure pulse is a very strong function of the inflow velocity $V_+ \simeq 0.5$ gives results in reasonable agreement with the experimen-

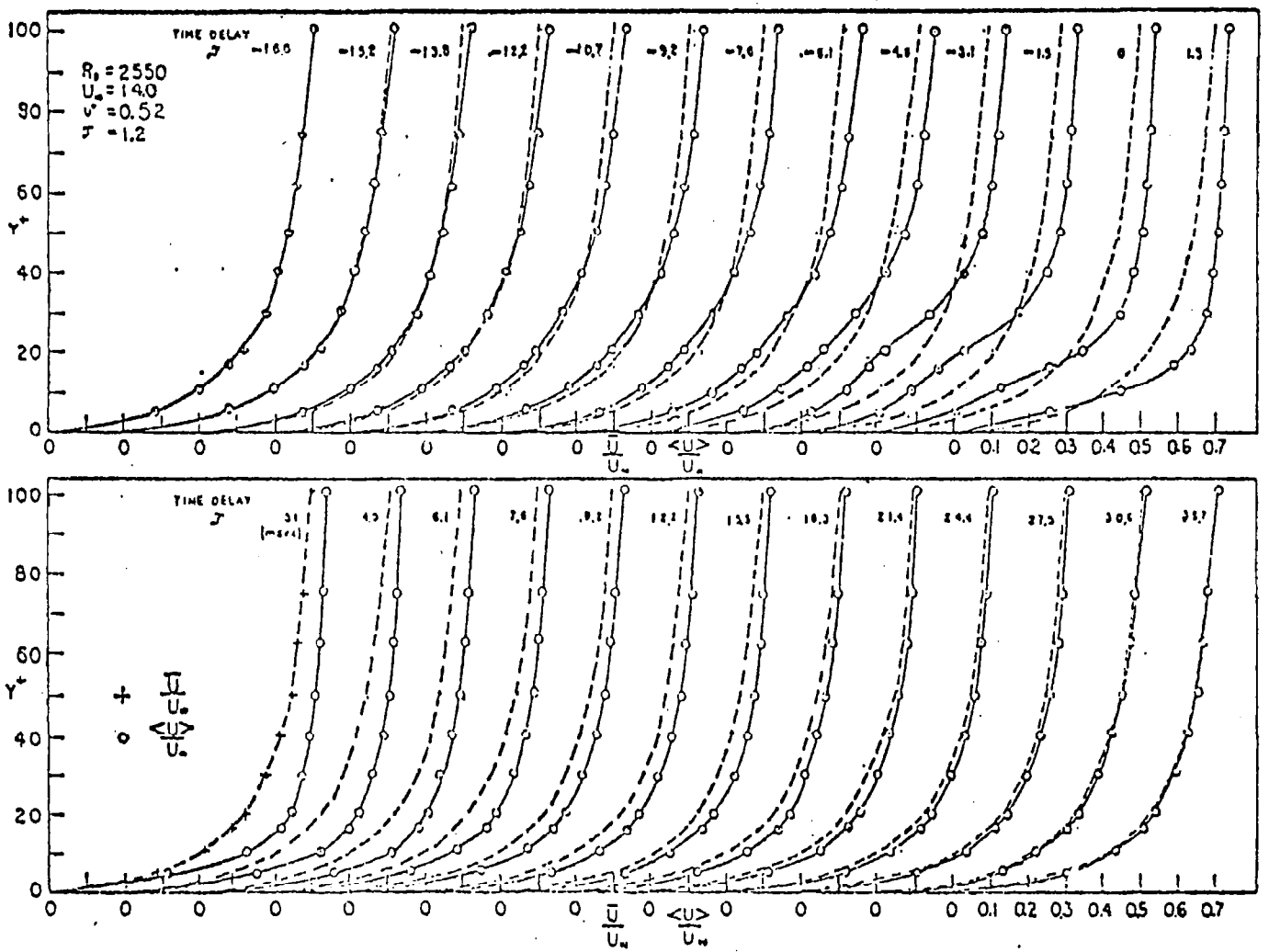

Figure 2. - Conditionally averaged and mean velocity profiles with positive and negative time delay from the point of detection, (From Ref. 20).

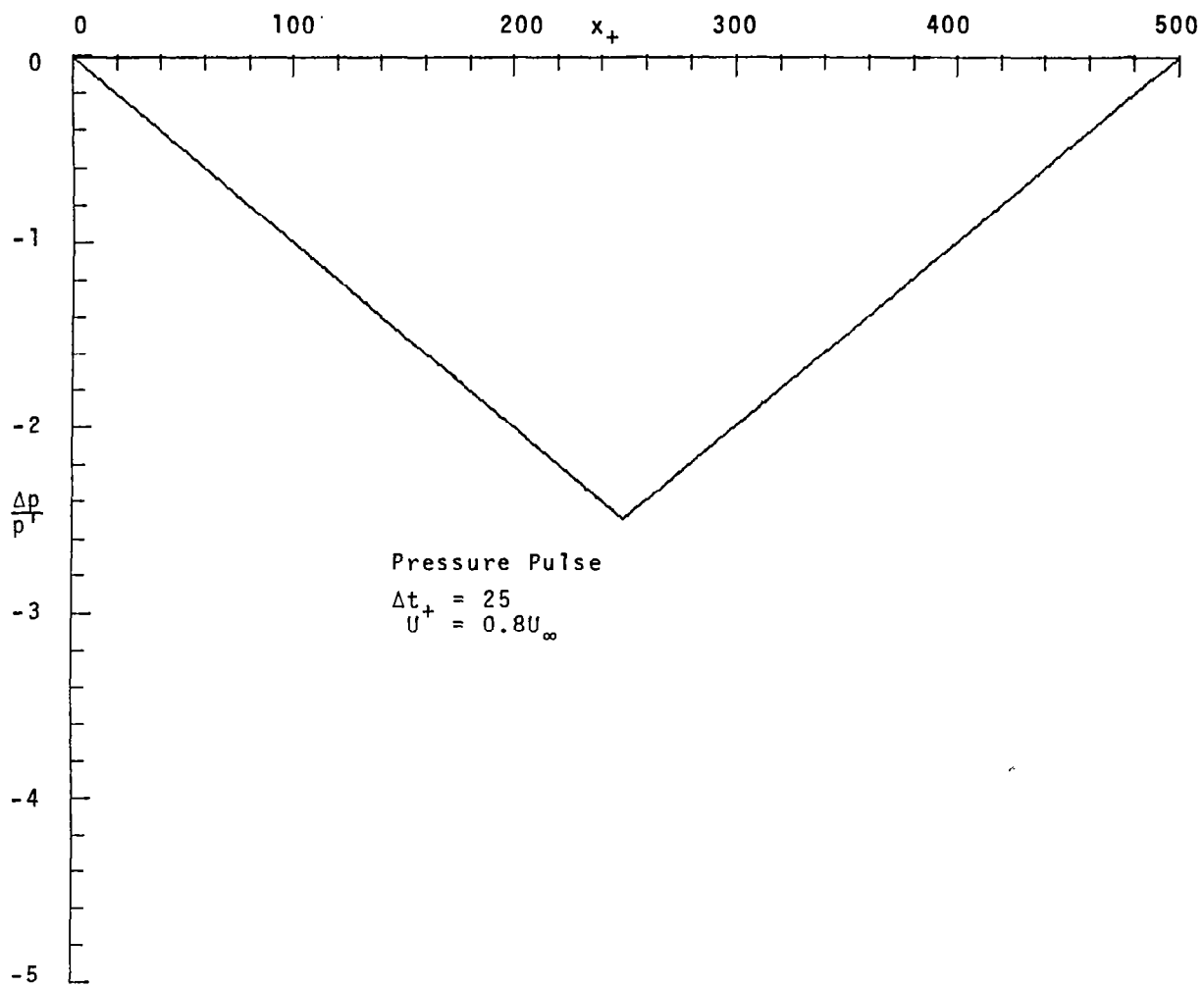

Figure 3. A plot of the imposed pressure pulse at $y_+ = H$. The form of this pulse is in good agreement with that measured by Burton.[4]

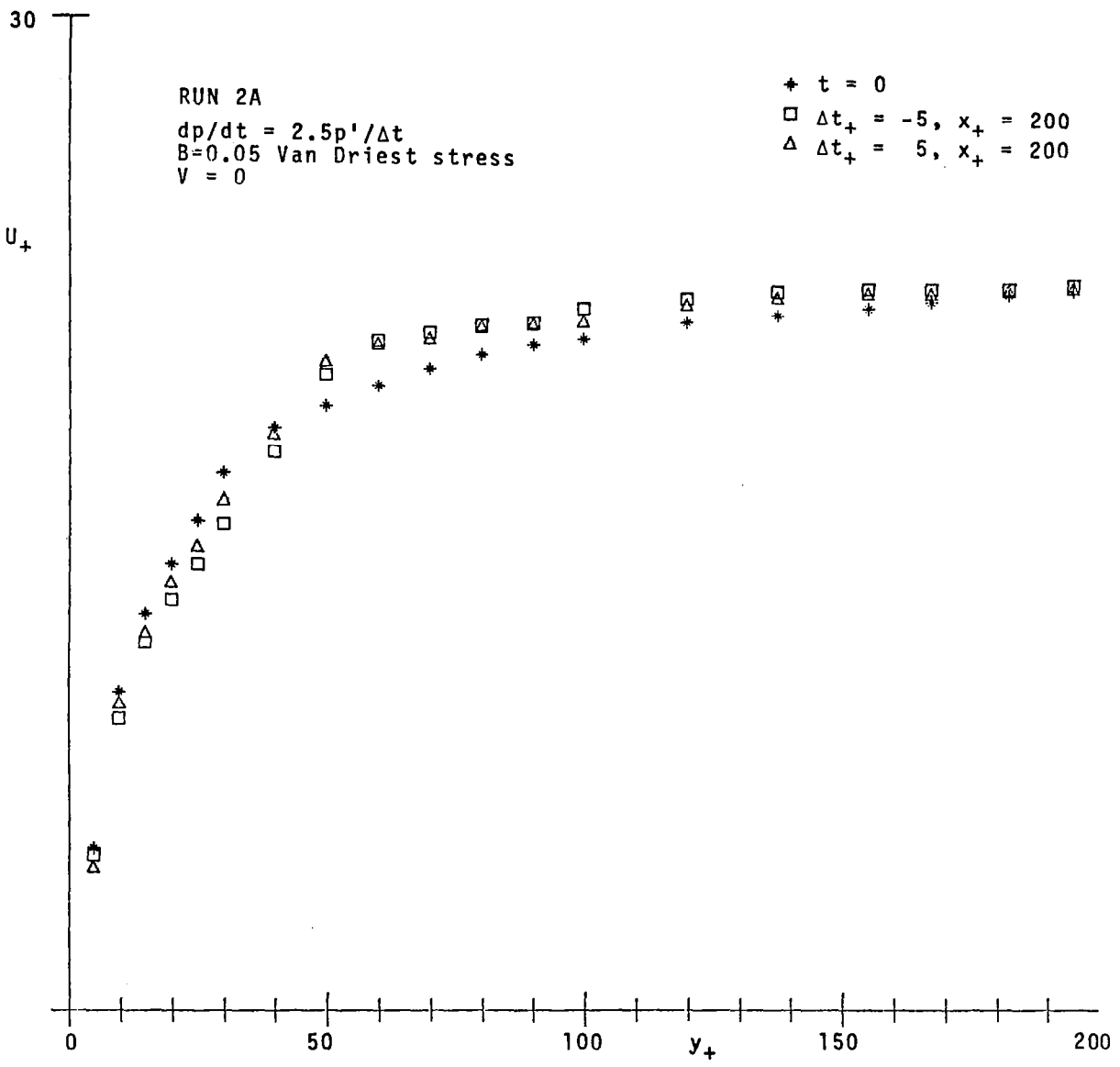

Figure 4. A plot of the calculated velocity profiles for Bushnell's model of the turbulent boundary layer. Time differences are measured from the peak of the adverse pressure gradient pulse. The boundary conditions at the top of the layer are v = 0.

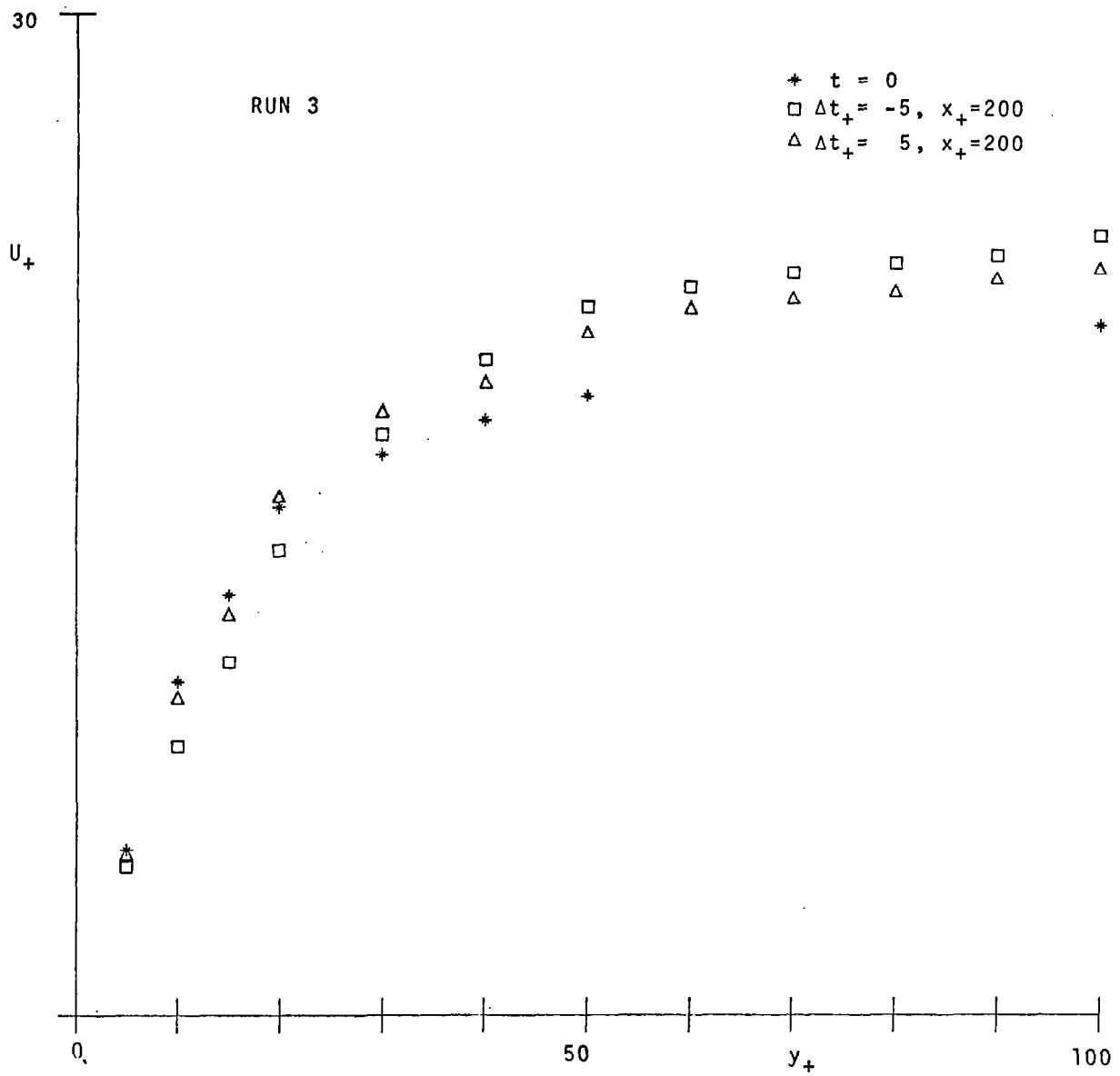

Figure 5. Same as Figure 4, except that the pressure pulse is applied at $y_+ = 100$ instead of $y_+ = 200$.

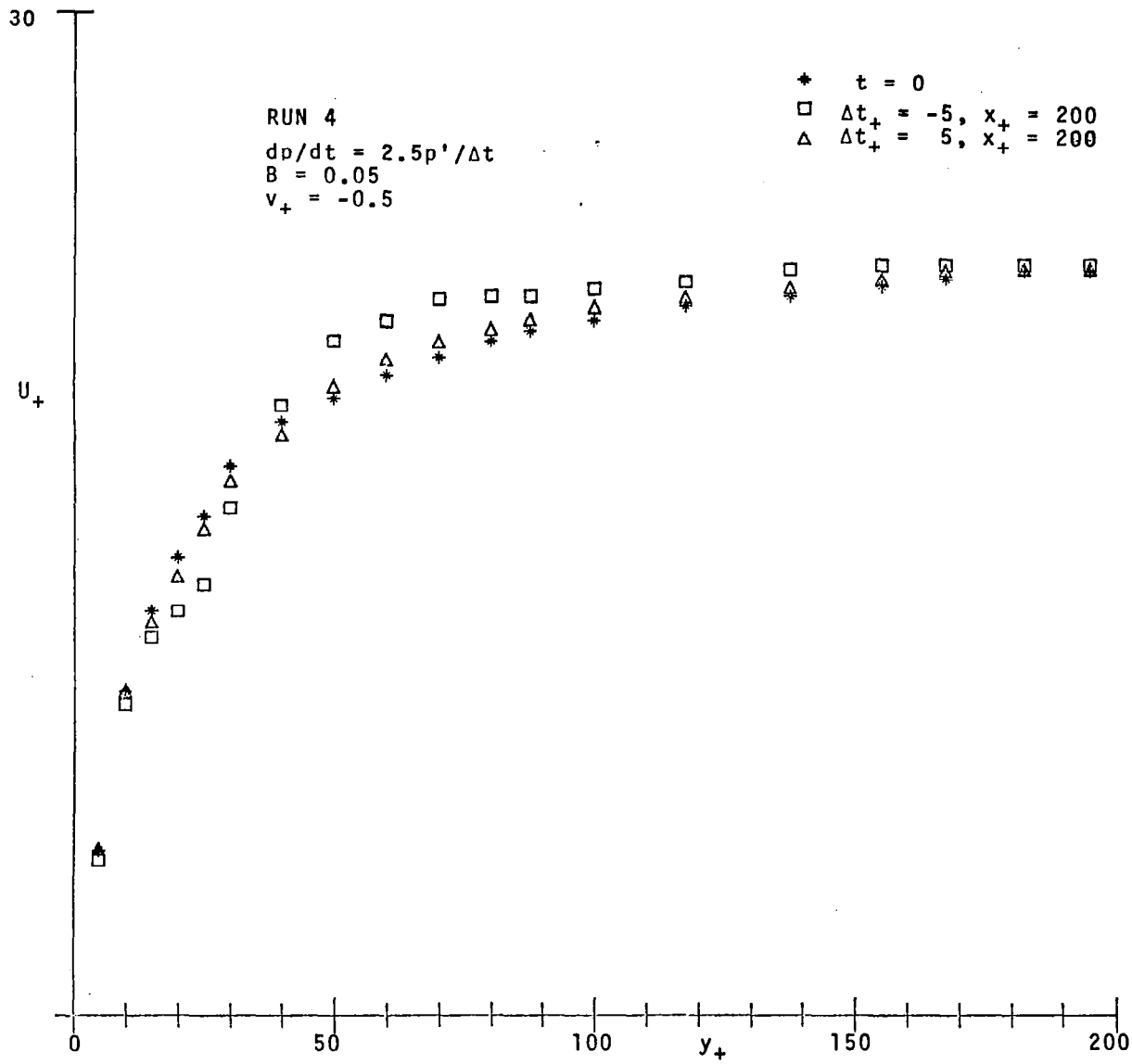

Figure 6. Same as Figure 4, except that an inflow velocity -0.5_+ is imposed at the top of the calculational domain $y_+ = 200$.

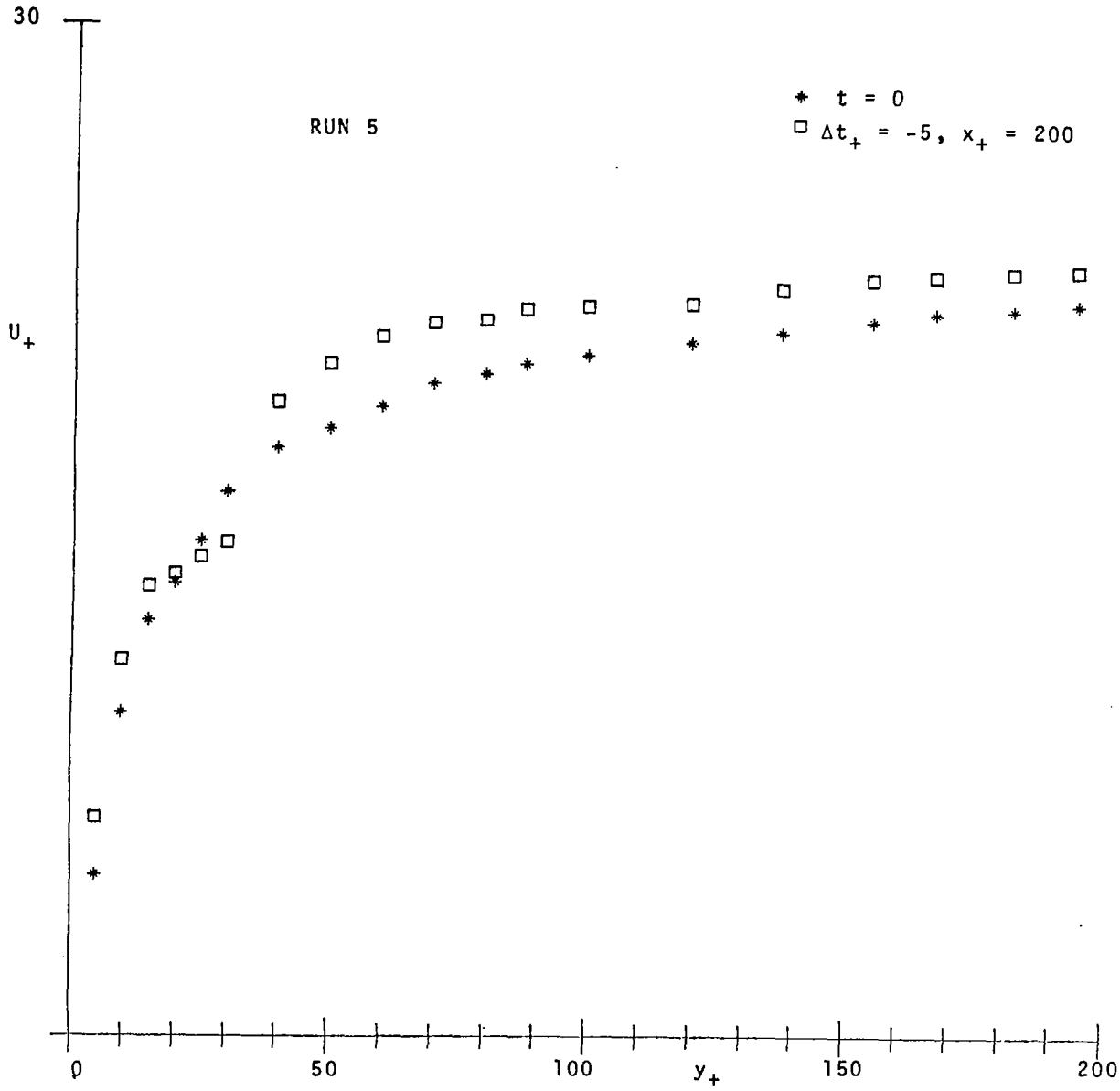

Figure 7. Same as Figure 4, except that an inflow velocity $V_+ = 2$ is imposed at the top of the calculational domain $y_+=200$.

tal data of Ref. 20.

6. COMPLIANT WALL RESULTS

We have performed about a dozen runs to study the effect of a compliant wall with imposed wall motion on the structure of a turbulent boundary layer. In all the experiments performed to date, we have assumed that the component of the wall motion in the direction of the mean flow vanishes: $U(x,t) = 0$. As discussed in Sec. 3, the justification for this approximation is that typical compliant boundaries have supports that stiffen the medium to lateral deformation. Our computer code has now run successfully in cases involving a wide variety of wavelengths of the wall motion. For very short and very long wavelength motions, stable results have been achieved with $H_+ = 200$, while we have had to use our variable grid map with $H_+ = 400$ to handle intermediate wavelength cases (see Sec. 3). For example, in Fig. 8, we plot the results of a numerical calculation for a flow over a compliant boundary whose surface motion was a short wave,

$$\eta(x,t)_+ = 5 \sin(2x_+ - 30t_+). \qquad (6.1)$$

This wave is as short as can be resolved on our grid with 257 grid points in x. (In fact, it is surely not resolved accurately on this grid, so the results for Run 7 are qualitatively correct at best.)

The characteristics of our compliant wall test runs reported here are listed in Table 1. For all runs but Run 7, $H_+ = 400$ and a variable grid map is used in y. In this Table, λ is the wavelength of the imposed sinusoidal wall motion, c is its phase speed, and A is its amplitude, all in sublayer (+) units.

TABLE 1. COMPLIANT WALL TEST MATRIX

Run	λ_+	c_+	A_+
7	3	15	5
10	30	15	5
11	20	20	5
12	60	15	5
13	30	10	5
14	20	10	5
15	40	10	5
16	40	10	10
17	40	20	5
18	40	20	15
19	80	15	5

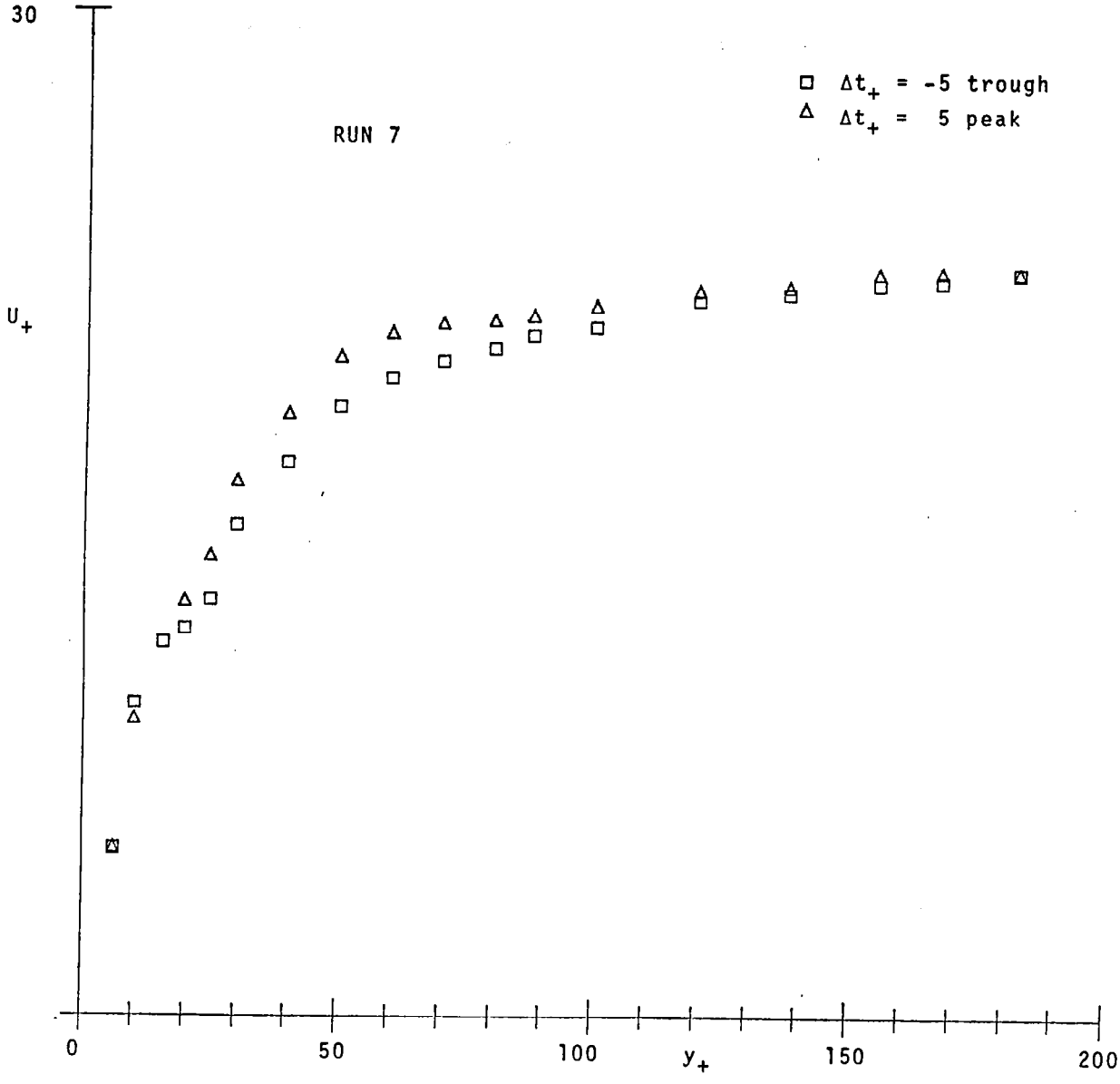

Figure 8. A plot of the calculated velocity profiles for Bushnell's model of the turbulent boundary layer over a moving wall. The imposed wall motion is a travelling sinusoid of amplitude $\eta_+ = 5$ and wavelength $\lambda_+ = \pi$ (short compared with the sublayer thickness).

We have performed stability calculations for these flows over compliant moving walls. The amplification ration A/A_0 is calculated as described in Sec. 4 for a wave that is initially most rapidly growing and the Michel-Smith correlation is used to predict the occurence of a burst. We assume that the drag on the turbulent boundary layer is proportional to the burst frequency, so that if the burst frequency is decreased then the drag is decreased proportionately.

In Fig. 9, we plot the amplification ratio vs. time for a wavepacket originating at $x_+ = 200$ for Runs 4 (Fig. 6) and 7 (Fig. 8), in order to demonstrate the effect of a compliant wall. In Fig. 9, we plot the data in two ways: the squares and triangles indicate the amplification factors obtained by local stability analysis following the most unstable wave using a phase speed transformation; the crosses and circles indicate the amplification factors obtained at a fixed location $x_+ = 200$, not following the wave.

The effect of the wall motion in decreasing the growth rate of disturbances in the boundary layer is apparent from the results plotted in Fig. 9 both following the wave and fixed in space. Also, the growth rates obtained following the wave are larger than those obtained fixed in space, apparently because when the wave packet moves it stays in a region of large amplification rate for a longer time and does not quickly encounter the favorable gradient part of the pressure pulse.

The results of our quasi-steady stability analyses of the runs tabulated in Table 1 are plotted in Fig. 10. The best result for a run in which the spatial resolution was adequate to give good results is for Run 14. It is disturbing that our results are so sensitive to the parameters of the wall motion. Perhaps the safest conclusion that can be made from these results is that drag reductions in excess of 25% or so may be available from compliant walls, but that the walls will have to be very carefully tuned to achieve such results.

In Figs. 11 and 12, we compare the results of a quasisteady analysis of Runs 13 and 14, respectively, with analysis based on the linearized Navier-Stokes equations. In Run 13, while the detailed growth rates are significantly different while the cumulative effect of the linearized stability analysis is quite well predicted by the quasi-steady analysis. On the other hand, in Run 14, the detailed growth rates are in reasonably good agreement while the cumulative error is somewhat larger. Until further verification of these results can be made by performing more runs, we must consider these results tentative and fortuitous. However, if quasisteady calculations prove uniformly good, major

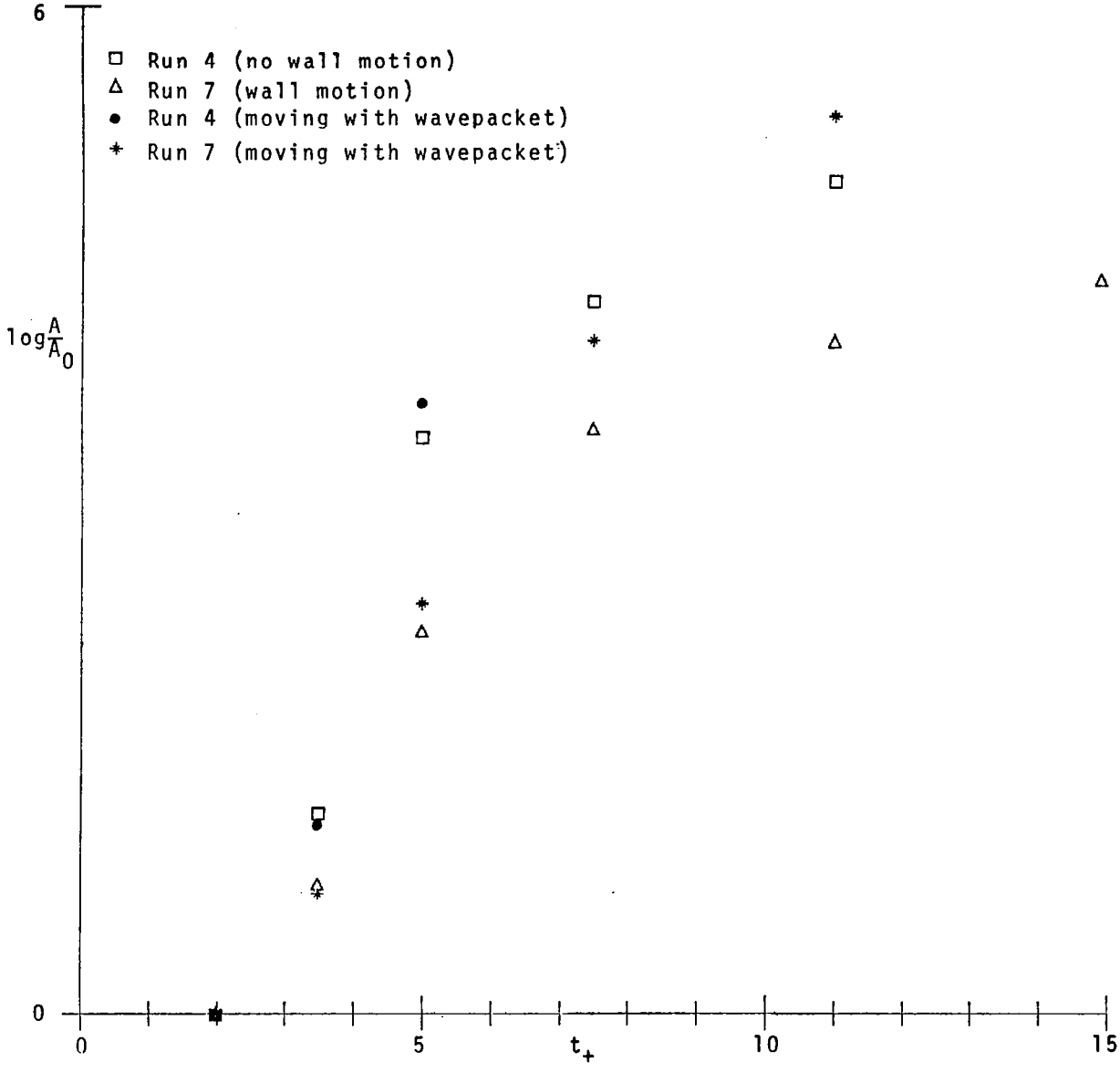

Figure 9. A plot of the amplification ratios of the most unstable disturbances of the boundary layer profiles of Runs 4 and 7, which are identical except that Run 7 has a short wavelength imposed wall motion. Results are presented for disturbances following the wavepacket and for disturbances fixed at $x_+ = 200$.

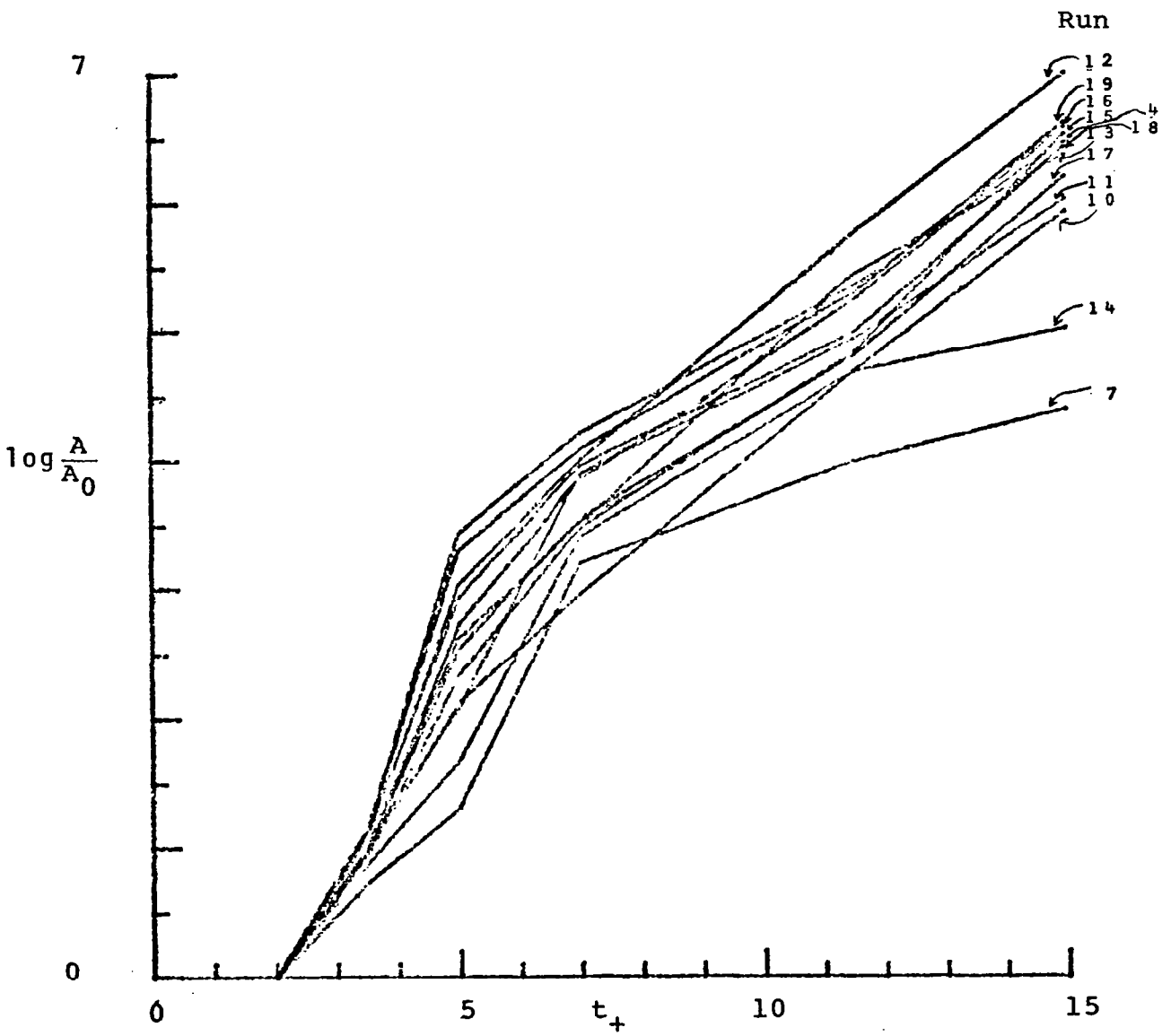

Figure 10. A plot of the results of quasi-steady stability analysis for the runs listed in Table 1. Note that Run 4 is for no wall motion. According to the Michel-Smith criterion for production of a burst, the burst frequency should be inversely proportional to the time required to achieve an amplification factor e^M with M of order 10. For all runs, the amplification factor is measured at $x_+=200$ in a fixed coordinate frame.

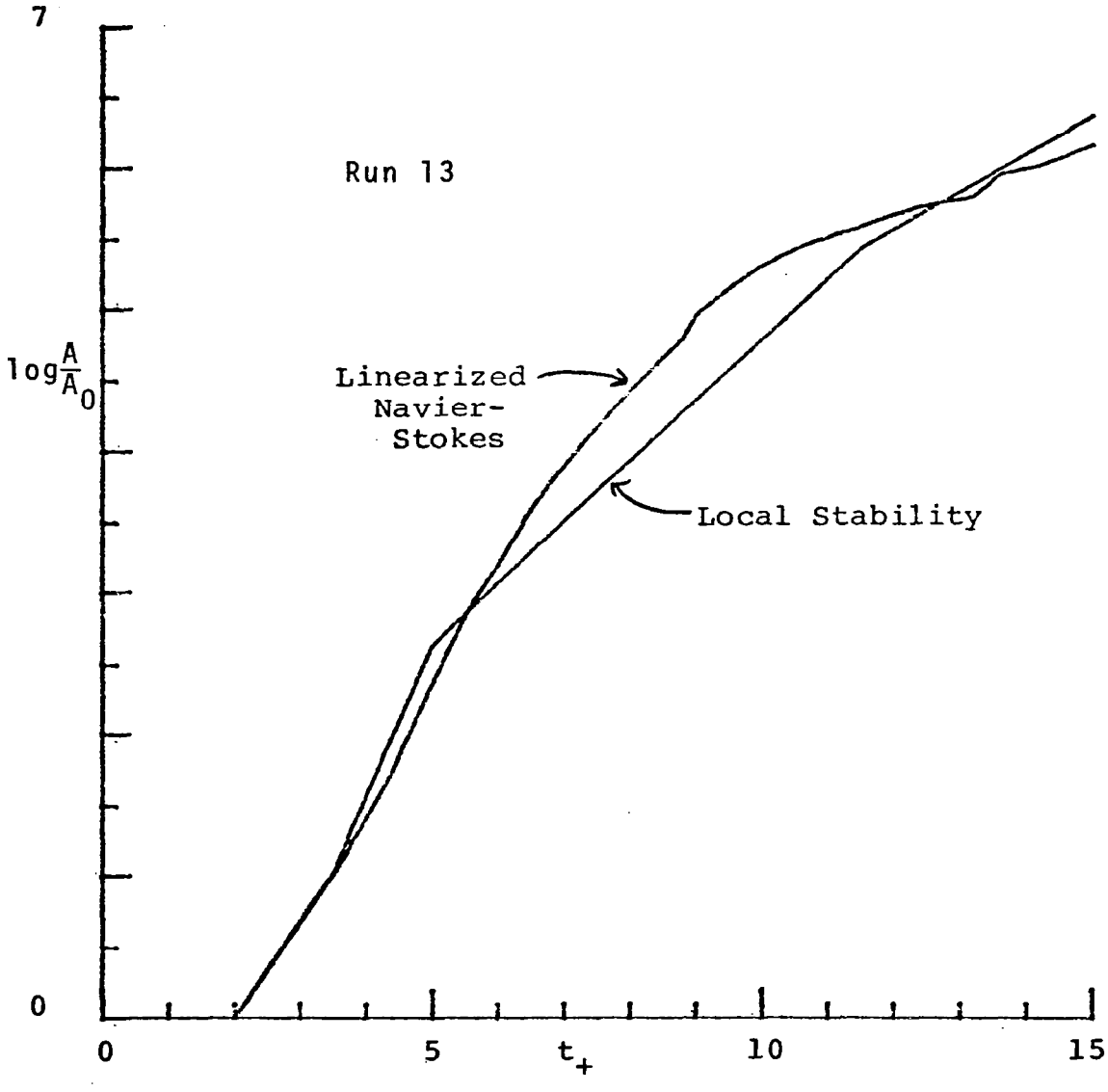

Figure 11. A comparison between the results of quasi-steady stability analysis using the Orr-Sommerfeld stability equation and the results of solution of the linearized Navier-Stokes equations (with periodic boundary conditions in x) for Run 13. The results are computed at $x_+ = 200$ in a coordinate frame fixed in space.

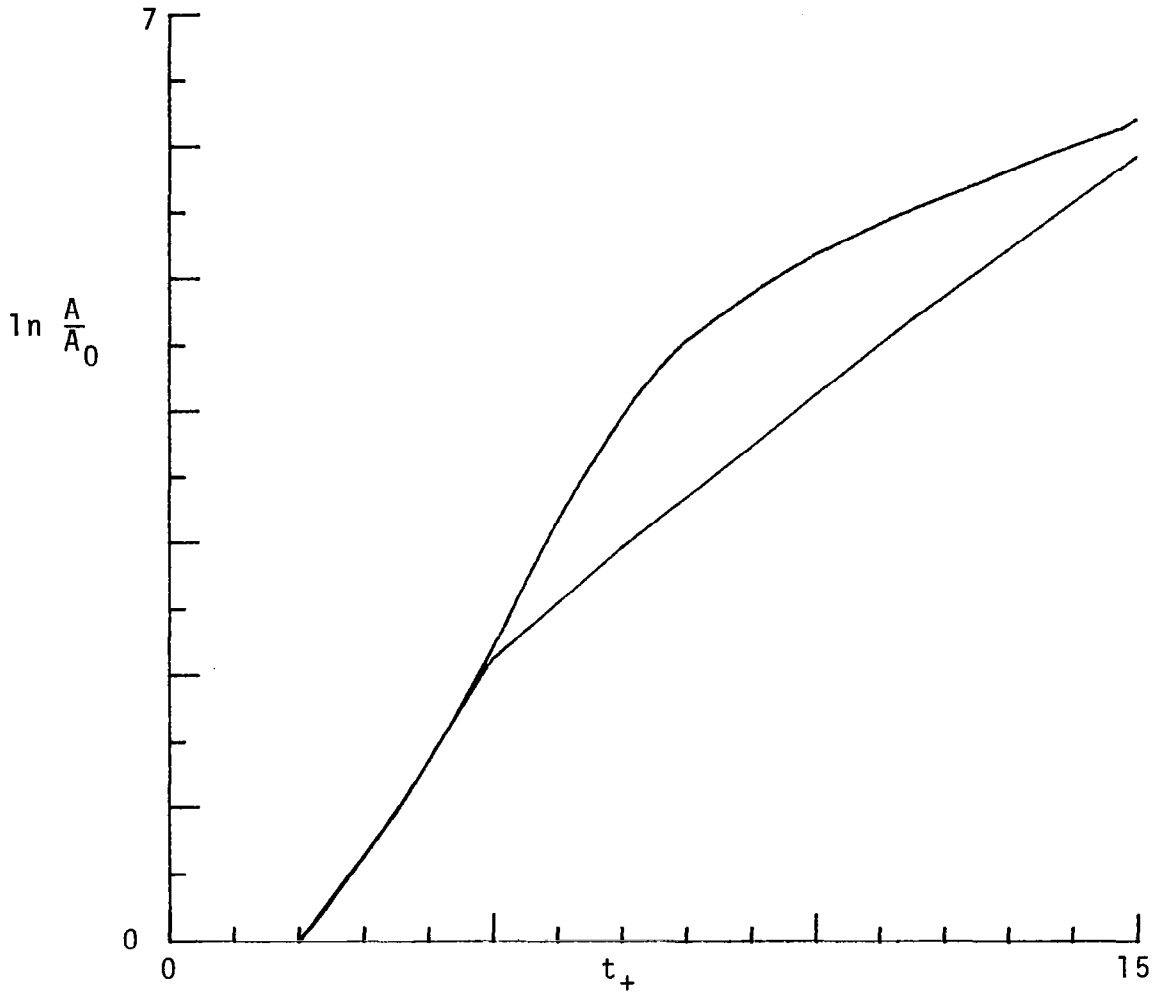

Figure 12. A comparison between the results of quasi-steady stability analysis using the Orr-Sommerfeld stability equation and the results of solution of the linearized Navier-Stokes equations (with periodic boundary conditions in x) for Run 14. The results are computed at $x_+ = 200$ in a coordinate frame fixed in space.

simplification of future calculations can result.

Similar calculations with even longer wavelengths have been performed. If the wavelength is of order the length of the pressure pulse, we have found drag enhancement of the order of 10-25%.

7. SUMMARY AND CONCLUSIONS

We have developed a set of computer codes to test Bushnell's boundary layer model. One code computes the evolution of mean velocity profiles during the period between bursts as forced by an imposed large-scale pressure pulse due to earlier bursts. Another code computes stability characteristics of these mean flows using the Orr-Sommerfeld stability equation. Still another stability code solves the linearized Navier-Stokes equations. Typical calculations involve the use of 33 Chebyshev polynomials to resolve the y direction and 257 grid points (or Fourier modes) to resolve the x-direction.

By carefully choosing the shape of the imposed pressure pulse, the level of the background turbulence, the height of the computational box, and, especially, the inflow velocity at the top of the boundary layer, we are able to achieve reasonable agreement with experimental measurements of mean velocity profiles during the burst process on a flat plate.

Stability calculations of the resulting mean velocity profiles show that compliant moving walls with relatively short wavelengths may have an appreciable effect in stabilizing the boundary layer to further bursts. On the other hand, long wavelength wall motions do not seem to limit the burst process, and therefore do not appear good candidates for drag reduction.

In future work on this problem, the effects of wall and stream curvature on the flow should be given added consideration. Some of these effects are included in the present calculation through the boundary conditions but their full effect on the turbulent boundary layer remains to be studied. In addition, the effects of three-dimensionality on these flows must be studied. As emphasized in Ref. 19, three-dimensional perturbations are frequently crucial in controlling the strong instabilities of planar shear flows.

REFERENCES

1. M. C. Fischer, L. M. Weinstein, R. L. Ash and D. M. Bushnell, "Compliant Wall-Turbulent Skin-Friction Reduction Research". AIAA Paper No. 75-833 (1975).

2. D. M. Bushnell, J. N. Hefner and R. L. Ash, "Compliant Wall Drag Reduction for Turbulent Boundary Layers". Phys. Fluids 20, S31 (1977).

3. M. O. Kramer, "Hydrodynamics of the Dolphin." Adv. in Hydroscience 2, 111 (1965).

4. T. E. Burton, "The Connection Between Intermittent Turbulent Activity Near the Wall of a Turbulent Boundary Layer with Pressure Fluctuations at the Wall." Sc. D. Thesis, M.I.T. (Cambridge, MA, 1974).

5. J. Laufer, "New Trends in Experimental Turbulence Reserach." Ann. Rev. Fluid Mech. 7, 307 (1975).

6. W. W. Willmarth, "Structure of Turbulence in Boundary Layers." Adv. in Appl. Mech. 15 (1975).

7. N. A. Jaffe, T. T. Okamura and A. M. O. Smith, "Determination of Spatial Amplification Factors and Their Application to Predicting Transition." AIAA Journal 8, 301 (1970).

8. S. A. Orszag, D. M. Bushnell and J. N. Hefner, "Model of Drag Reduction by Compliant Walls." Phys. Fluids 20, S289 (1977).

9. E. R. Van Driest, "On Turbulent Flow Near a Wall." J. Aero. Sci. 23, 1007 (1956).

10. S. A. Orszag, "Prediction of Compliant Wall Drag Reduction-Part I." NASA CR-2911 (1977).

11. C. E. Grosch and S. A. Orszag, "Numerical Solution of Problems in Unbounded Regions: Coordinate Transforms." J. Comp. Phys. 25, 273 (1977).

12. S. A. Orszag and M. Israeli, "Numerical Simulation of Viscous Incompressible Flows." Ann. Rev. Fluid Mech. 6, 281 (1974).

13. D. Gottlieb and S. A. Orszag, Numerical Analysis of Spectral Methods· Theory and Applications. NSF-CBMS Monograph No. 26, SIAM (Phila., PA, 1977).

14. S. A. Orszag, "Fourier Series on Spheres." Mon. Weather Rev. 102, 56 (1974).

15. A. Michalke, "On Spatially Growing Disturbances in an Inviscid Layer." J. Fluid Mech. 23, 521 (1965).

16. S. A. Orszag, "Accurate Solution of the Orr-Sommerfeld Stability Equation." J. Fluid Mech. 50, 689 (1971).

17. D. J. Benney and S. A. Orszag, "Stability Analysis for Laminar Flow Control - Part I." NASA CR-2910 (1977).

18. A. Srokowski and S. A. Orszag, "Mass Flow Requirements for LFC Wing Design." AIAA Paper No. 77-1222 (1977).

19. S. A. Orszag and L. Kells, "Transition to Turbulence in Plane Poiseuille and Plane Couette Flow." CHI Report #10 (1978).

20. R. F. Blackwelder and R. E. Kaplan, "On the Wall Structure of the Turbulent Boundary Layer." J. Fluid Mech. 76, 89 (1976).

1. Report No.	2. Government Accession No.	3. Recipient's Catalog No.
NASA CR-3071		

4. Title and Subtitle	5. Report Date
Prediction of Compliant Wall Drag Reduction - Part II	December 1978
	6. Performing Organization Code

7. Author(s)	8. Performing Organization Report No.
Steven A. Orszag	
	10. Work Unit No.

9. Performing Organization Name and Address	11. Contract or Grant No.
Cambridge Hydrodynamics, Inc. P. O. Box 249, MIT Station Cambridge, MA 02139	NAS1-14906
	13. Type of Report and Period Covered
12. Sponsoring Agency Name and Address	Contractor Report
National Aeronautics and Space Administration Washington, DC 20546	14. Sponsoring Agency Code

15. Supplementary Notes

Langley Technical Monitor: Jerry N. Hefner

Final Report

16. Abstract

A numerical model of turbulent boundary layer flows over compliant walls has been investigated. The model is based on Burton's observation that outer flow structures in turbulent boundary layers produce large scale pressure fluctuations near the wall. The results of our calculations indicate that certain small wavelength wall motions can have a significant effect upon the stability of turbulent boundary layers.

17. Key Words (Suggested by Author(s))	18. Distribution Statement
Drag reduction Compliant walls Navier-Stokes equations Turbulence model Numerical methods Spectral methods	Unclassified - Unlimited Subject Category 34

19. Security Classif. (of this report)	20. Security Classif. (of this page)	21. No. of Pages	22. Price*
Unclassified	Unclassified	28	$4.50

* For sale by the National Technical Information Service, Springfield, Virginia 22161

NASA-Langley, 1979